26th EPS Conf. on Contr. Fusion and Plasma Physics, Maastricht, 14 - 18 June 1999 ECA Vol.23J (1999) 421 - 424

Monte Carlo Simulation of Particle and Heat Transport in Internal Transport Barrier

K.Hamamatsu, T.Takizuka, H.Shirai, Y.Kishimoto, C.S.Chang*

Naka Fusion Research Establishment, Japan Atomic Energy Research Institute, Naka, Ibaraki, 311-0193, Japan
**Courant Institute of Mathematical Sciences, New York University, 251 Mercer street, New York, NY10012, USA*

1. Introduction

Many types of internal transport barrier (ITB) have been observed in many tokamaks. Recently, a quasi steady ITB has been obtained in the reversed magnetic shear operation of JT-60U[1]. The ITB observed in JT-60U has steep gradients of electron temperature T_e, ion temperature T_i and electron density n_e, where thermal and particle transport is significantly reduced. The width of some ITBs becomes around 5∼10 cm where the scale length is comparable to the ion poloidal Larmor radius. A strong radial electric field is also observed around the ITB layer, which is evaluated at about −50kV/m. The ion and electron thermal diffusivities evaluated by experimental observation are considered to be reduced down to the same level predicted by the neoclassical theory.

Many ions around the ITB layer pass through the ITB due to a large orbit width. These ions experience different collisionality inside and outside of the ITB and are affected by the radial electric field. Such a situation suggests that a conventional neoclassical theory is hardly applied. In this paper, the effects of finite orbit width and radial electric field on ion transport are analyzed by using the orbit following Monte Carlo (OFMC) code[2].

2. Effects of electric field on particle orbit

We start from the conservation law for the energy E, canonical angular momentum P_ϕ and magnetic moment μ, where the poloidal flux function ψ and the electrostatic potential ϕ are given as functions of minor radius r. After straightforward calculation under the assumption of circular magnetic surface, we obtain the orbit equations:

$$\left(\frac{\bar{P}_\phi - \Psi}{1+\epsilon\cos\theta}\right)^2 + \frac{\bar{\mu}}{1+\epsilon\cos\theta} = \bar{E} - \Phi \quad , \quad v_\parallel = \frac{\bar{P}_\phi - \Psi}{1+\epsilon\cos\theta} \tag{1}$$

where $\Psi = q\psi(r)/(mR_{\rm ax})$, $\Phi = 2q\phi(r)/m$, $\bar{E} = 2E/m$, $\bar{\mu} = 2\mu B_{\rm ax}/m$, $\epsilon = r/R_{\rm ax}$, $R_{\rm ax}$ is the major radius, m is the mass, $B_{\rm ax}$ is the magnetic field at $R = R_{\rm ax}$, θ is the poloidal angle and $v_\parallel$ is the parallel velocity. The pitch angle region of trapped particle is obtained from Eq.(1). In the case of the negative electric field ($E_{r0} < 0$), the region is

$$-\sqrt{2\epsilon_0} - U_{\rm E0}(1-2\epsilon_0) \leqq v_{\parallel_0}/v_0 \leqq 0 \quad \text{and} \quad -2U_{\rm E0} \leqq v_{\parallel_0}/v_0 \leqq \sqrt{2\epsilon_0} - U_{\rm E0}(1-2\epsilon_0) \tag{2}$$

where $U_{\rm E0} = V_{\rm E0}/v_0$, $V_{\rm E0} = E_{r0}/B_{\rm p0}$ and $B_{\rm p0}$ is poloidal magnetic field. Here, the suffix "0" means the quantity on the equatorial plane in the low field side. The banana width is also evaluated as

$$\Delta_{\rm B} = 2\left(\rho_{\rm p\parallel 0} + U_{\rm E0}\frac{v_0}{\Omega_{\rm p0}}\right)\left(1 - \frac{\rho_{\rm p\parallel 0}}{r_0}\right) \tag{3}$$

where $\rho_{\mathrm{p}\|0} = v_{\|_0}/\Omega_{\mathrm{p}0}$ and $\Omega_{\mathrm{p}0} = qB_{\mathrm{p}0}/m$. In the derivation of Eqs.(2) and (3), we use the following assumption: $\epsilon_0 \ll 1$, $\rho_{\mathrm{p}\|0}/r_0 \ll 1$ and $|U_{\mathrm{E}0}| \ll 1$. The Eq.(2) shows that the trapped particle region is separated into two regions. The mid-region ($0 < v_{\|_0}/v_0 < -2U_{\mathrm{E}0}$) is occupied by transit banana particles. The banana width of the transit banana particle changes the sign at $v_{\|_0} = -U_{\mathrm{E}0}v_0$ (see Eq.(3)). The radial electric field makes the inward transit banana particles in the region of $0 < v_{\|_0}/v_0 < -U_{\mathrm{E}0}$.

In the numerical calculation, we follow the guiding center motion:

$$\frac{\mathrm{d}v_{\|}}{\mathrm{d}t} = -\frac{\mu}{m}\frac{\partial B}{\partial \ell} + \frac{v_{\|}}{B^3}\boldsymbol{B}\cdot(\boldsymbol{\nabla}B\times\boldsymbol{E}), \quad \boldsymbol{v}_{G\perp} = \frac{\boldsymbol{E}\times\boldsymbol{B}}{B^2} + \frac{1}{q}\left(\mu + \frac{mv_{\|}^2}{B}\right)\frac{\boldsymbol{B}}{B}\times\frac{\boldsymbol{\nabla}B}{B} \qquad (4)$$

where $\boldsymbol{v}_{G\perp}$ is the drift velocity perpendicular to the magnetic field, $\boldsymbol{B}$ is the static magnetic field, ℓ is the arc length along the magnetic field line. Figure 1 shows numerical results obtained in the JT-60U configuration, where the particle energy is $mv_0^2/2 \sim 5$keV, $R_{\mathrm{ax}} \sim 3.4$m, $B_{\mathrm{T}} \sim 3.8$T, $I_{\mathrm{p}} \sim 1.5$MA, $a \sim 0.8$m and $\kappa \sim 1.6$. Figure 1.(a) is the case of week electric field ($E_{r0} \sim -10$kV/m) and $r_0 \sim 0.49$m. The orbit width is draw in the upper side for a given particle energy. In the lower side of figure, the inward transit banana and trapped banana regions are shown by the dark and pale shaded regions, respectively. The strong electric field case ($E_{r0} \sim -50$kV/m) is shown in Fig.1(b), where $r_0 \sim 0.46$m. The population of inward transit banana increases. The strength of electric field used in Fig.1(a) and (b) corresponds to the center and edge region of ITB, respectively. The maximum banana width does not so much change around 0.05 in the both cases. The banana particle may experience the velocity space, which changes between Fig.1(a) and (b). At the same, the particle is affected by the Coulomb collision. Figure 2 shows the typical orbit of the inward transit banana, which corresponds to $\cos^{-1}(v_{\|_0}/v_0) = 89°$ and $v = v_0$ in Fig.1(b). The orbit projected on the poloidal plane is shown in Fig.2(a), where the starting point is indicated by the symbol '×'. The poloidal position along the toroidal direction ζ is shown in the Fig.2(b). To investigate the particle and energy transport, we perform the Monte Carlo simulation.

3. Simulation model

We assume for simplicity that the plasma is Maxwellian and uniform along the magnetic surface. The radial profiles of temperature and density are given by functions of radial coordinate ρ. The radial coordinate is defined by $\rho = \sqrt{V(\psi)/V(\psi_{\mathrm{s}})}$, where V is the volume surrounded by the magnetic surface and ψ_{s} shows the most outer surface.

The transport coefficients are obtained by observing the propagation of particle and energy pulses. In this study, we evaluate the transport coefficients of the test particles not of the total plasma. As an initial condition, test ions are distributed uniformly along the magnetic surface of $\rho = \rho_0$, where velocities are distributed as Maxwellian with bulk ion temperature $T_{\mathrm{i}}(\rho_0)$. The ion motion is simulated by guiding center motion, i.e., Eq.(4). Coulomb collision effects, i.e., slowing down, pitch angle scattering and energy diffusion effects, are simulated from a Monte Carlo technique. Numerical simulation is performed by using the OFMC code. Trajectories of ions in the phase space give a distribution function $f(\rho, \boldsymbol{v}, t)$. The particle and energy densities, $n(\rho, t)$ and $e(\rho, t)$, are defined as

$$n(\rho,t) = \int \mathrm{d}\boldsymbol{v} f(\rho,\boldsymbol{v},t) \quad , \quad e(\rho,t) = \int \mathrm{d}\boldsymbol{v}\left[\frac{m}{2}v^2 + q\Big(\phi(\rho) - \phi(\rho_0)\Big)\right] f(\rho,\boldsymbol{v},t), \qquad (5)$$

where the electrostatic potential is included to satisfy the energy conservation law. The time evolutions of $n(\rho, t)$ and $e(\rho, t)$, which are obtained by the OFMC, are assumed to

be described by the following equations

$$\frac{\partial}{\partial t}n(\rho,t) = -\frac{1}{\rho}\frac{\partial}{\partial \rho}\left[\rho\left\{-D^{\rm p}(\rho)\frac{\partial n(\rho,t)}{\partial \rho}+F^{\rm p}(\rho)n(\rho,t)\right\}\right] \quad (6)$$

$$\frac{\partial}{\partial t}e(\rho,t) = -\frac{1}{\rho}\frac{\partial}{\partial \rho}\left[\rho\left\{-D^{\rm e}(\rho)\frac{\partial e(\rho,t)}{\partial \rho}+F^{\rm e}(\rho)e(\rho,t)\right\}\right]+s_{\rm col}(\rho,t), \quad (7)$$

where $s_{\rm col}(\rho,t)=(m/2)\int {\rm d}\boldsymbol{v}v^2C(f(\rho,\boldsymbol{v},t))$ is a source and/or sink term of energy due to the Coulomb collision. The time evolution of $s_{\rm col}$ is also obtained by the OFMC code. The diffusion and flow coefficients, $D^{\rm p}, D^{\rm e}, F^{\rm p}, F^{\rm e}$, are numerically evaluated from the k-th radial moments of n, e and $s_{\rm col}$, i.e., $\int_0^1 {\rm d}\rho\rho^k n(\rho,t)$ and so on.

4. Numerical results

The simulations are performed in plasmas with a typical ITB configuration of JT-60U. The plasma consists of electrons, protons and carbon impurities (Z=6). The profiles of plasma, electrostatic potential and safety factor q_s are shown in Fig.3. The impurity profile is assumed to be the same as that of electron and Zeff=3. The temperature of impurities is the same as bulk-proton temperature. In Fig.3(c), the minimum value of electric field, $E_{r\min}$, is set at -50kV/m at $\rho=0.6$.

In Fig.4, the transport coefficients of energy for $E_{r\min}=0,-50$ and -100 kV/m are shown by the solid, dashed and dotted line, respectively. The minimum electric field $E_{r\min}=-100$kV/m is changed by the absolute value of ϕ. In these simulations, 4×10^4 particles are used. The diffusion coefficient is shown in Fig.4(a). The spatial profiles of diffusion coefficient are similar and strongly depend on the square of banana width. The flow coefficient is described in Fig.4(b). In the case of $E_r=0$, the energy flow is not induced, where the fluctuation is in the noise level. The outward flow is caused around the strong electric field near $\rho\sim0.6$ and the inward flow is induced in the week electric field regions of both sides of the strong electric field. The velocity spaces shown in Fig.1 (a) and (b) just correspond to two positions of $\rho\sim0.6$ and $\rho\sim0.65$. The transport coefficients of particle are also similar dependence of the energy transport.

5. Summary and Discussion

The obtained results show that the diffusion is not so much changed by the radial electric field. The reduction of transport at the ITB can be caused by the inward flow related to the radial electric field. We consider the transport of total energy, which includes the electrostatic potential, to satisfy the energy conservation law. When the energy flow is induced, we must take account of the exchange between the kinetic energy and the potential energy, which is related to the particle transport.

In this paper, the distribution function of bulk ions is fixed, i.e., the momentum and energy of the whole plasma are not conserved in the used Coulomb collision model. A simulation method to obtain the transport coefficients of the total plasma is now under discussion. Furthermore, the consistency between the electric field and the transport is not considered. It is left to a future work.

References

[1]S.Ishida et al, Plasma Physics and Controlled Nuclear Fusion Research, Yokohama 1998 (International Atomic Energy Agency, Vienna), IAEA-CN-69/OV1/1

[2]K.Tani et al, J. Phys. Soc. Jpn. 50 (1981) 1726

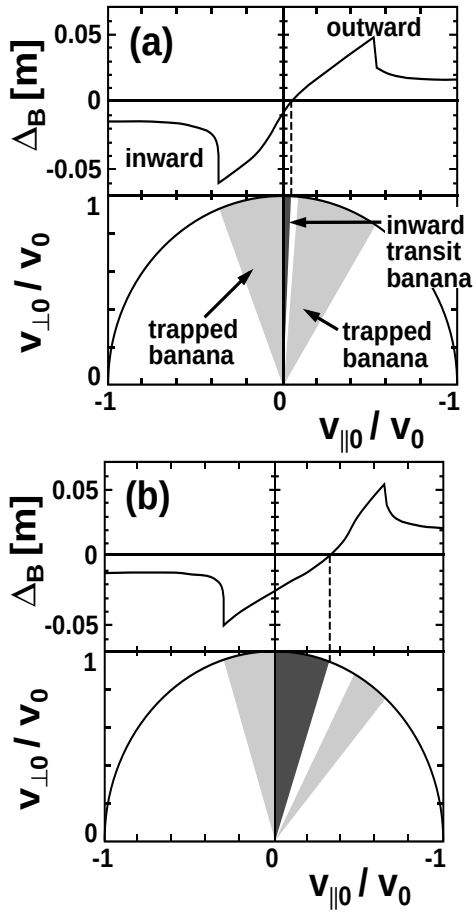

Fig.1 Orbit width and inward transit banana shown in the velocity space.

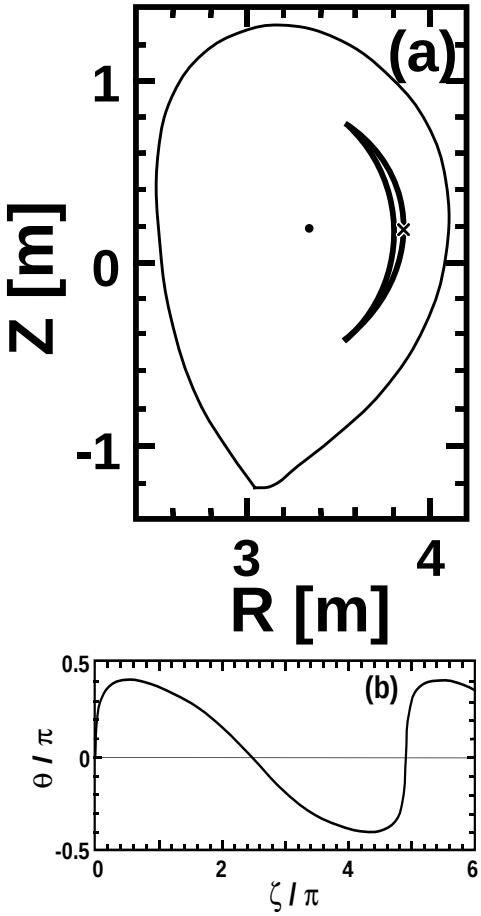

Fig.2 Orbit of inward tranzit banana.

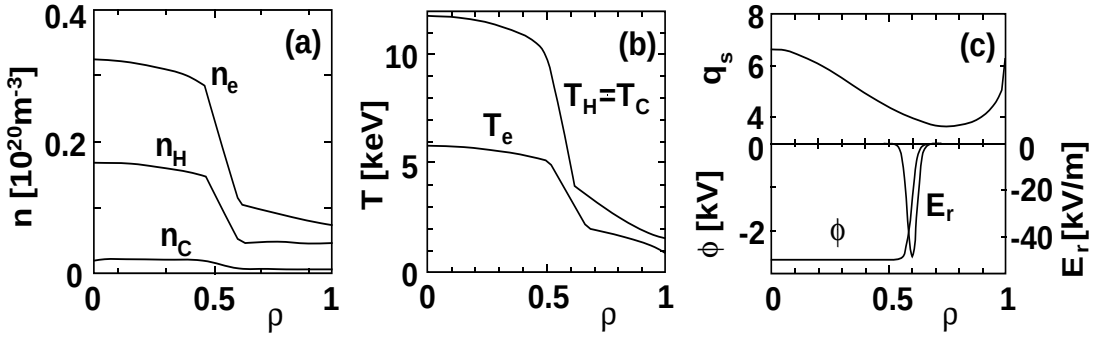

Fig.3 Plasma and field profiles used in the Monte Carlo simulation.

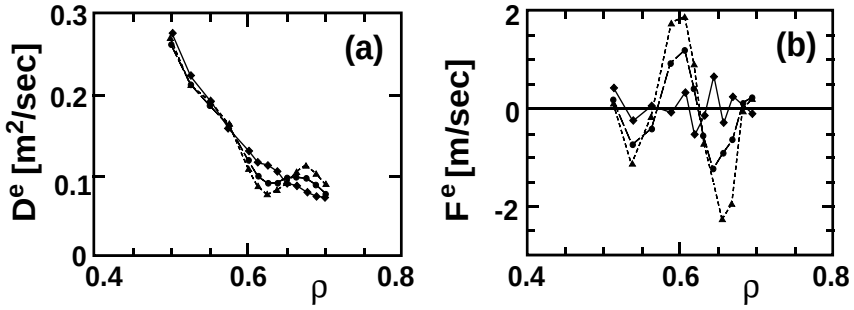

Fig.4 Transport coefficients of energy.